Supplementary Materials

The Synchronization of Electron Enricher and Electron Extractor as Ternary Composite Photoanode for Enhancement of DSSC Performance†

Weradesh Sangkhun,[1] Sompit Wanwong,[1,2] Nutthapon Wongyao,[3] Teera Butburee,[4] Pisist Kumnorkaew,[4] Jatuphorn Wootthikanokkhan,[1,2*]

[1] Division of Materials Technology, School of Energy, Environment and Materials, King Mongkut's University of Technology Thonburi (KMUTT), Bangkok, 10140, Thailand.
[2] Nanotec−KMUTT Center of Excellence on Hybrid Nanomaterials for Alternative Energy (HyNAE), School of Energy, Environment and Materials, King Mongkut's University of Technology Thonburi, Bangkok, 10140, Thailand.
[3] Fuel Cells and Hydrogen Research and Engineering Center, King Mongkut's University of Technology Thonburi, Bangkok, 10140, Thailand.
[4] National Nanotechnology Center, National Science and Technology Development Agency, Thailand Science Park, Pathum Thani, 12120, Thailand.

Correspondence should be addressed to Jatuphorn Wootthikanokkhan; jatuphorn.woo@kmutt.ac.th

S1: Materials, Synthesis and Characterizations

S1.1 Materials

Graphite powder, (synthetic grade, <20 μm), acetonitrile (99.8% anhydrous), *tert*-butanol (≥99.5% anhydrous), titanium (IV) isopropoxide (≥97.0%, TTIP), and FTO substrate (fluorine doped tin oxide, sheet resistance ~7 Ω/cm^2) were obtained from Sigma Aldrich. Hydrofluoric acid, (48% AR grade) was purchased from VWR Chemicals. Sodium nitrate (99.0%) and potassium permanganate (99.0%) were obtained from Ajax Finechem. Ethanol (absolute), sulfuric acid (95–97% AR grade), hydrochloric acid (fuming, 37%), Thiourea (≥99.0%), and acetic acid (100% glacial) were obtained from Merck. 2-Propanol (≥99.9% AR grade, IPA) and sodium hydroxide (98% anhydrous) was supplied by Carlo Erba**.** Tetrabutyl orthotitanate (TBOT) (≥97% AR grade) was obtained from Fluka**.** Deionized water (pH 6.2, 0.8 μΩ/cm) was supplied by Siam Beta. TiO_2 nano-powder (P25, 21 ± 10 nm), were supplied by Plasma Chem (Germany). N719 dye (Ruthenizer 535−bisTBA), electrolyte solution (Iodolyte HI–30), platinum paste (Platisol T/SP), and silver paste (Elcosil S−L/SP) were purchased from Solaronix. A sealing film based on ethylene acrylic acid copolymer (Surlyn® thermoplastic resin) was purchased from Dupont®. Nitrogen gas (99.999%) was supplied from Praxair. Unless specified, all chemicals were used as received.

S1.2 Synthesis of $TiO_{2\{001\}}$ and N, S doped $TiO_{2\{001\}}$

The TiO_2 with exposed {001} facet was synthesized by using a hydrothermal method. The reaction was carried out at 10 °C, under nitrogen atmosphere (99.999%, Praxair) by using Schlenk line technique. Practically, the synthesis was commenced by adding 46 mL of water, 14.5 mL of HCl (37%), 1.5 mL of acetic acid, and 1 mL of TBOT. The content in the reaction flask was stirred at ~10 °C for 3 h under nitrogen gas. Next, the product was transferred into a stainless-steel autoclave and reaction process was carried out at 200 °C for 12 h. After that, the product was centrifuged at 6,000 rpm for 30 min. The isolated precipitate was then washed with ethanol followed by deionized water, until the pH value was neutral. The powder was then dried in a vacuum oven at 60 °C for 24 h. Finally, the dried $TiO_{2\{001\}}$ powder was calcined at 500 °C for 3 h under atmospheric condition. To obtain TiO_2 crystals with different percentage of {001} facet, the molar ratios between HF and Ti were varied accordingly; HF/Ti = 1 ($TiO_{2\{001\}}$-1F), HF/Ti = 2 ($TiO_{2\{001\}}$-2F), HF/Ti = 3 ($TiO_{2\{001\}}$-3F), and HF/Ti = 4 ($TiO_{2\{001\}}$-4F). For N, S doped $TiO_{2\{001\}}$ synthesis, 200 μL of 1 M thiourea solution was slowly dropwised into the solution at 2 h of stirring time and then continuously stirred for another 1 h.

S1.3 Synthesis of GO and N, S doped rGO

The GOs were synthesized by the modified Hummer's method under three different conditions, which are (i) the low temperature condition (GO-(LT)), (ii) the high temperature condition (also known as a conventional method) (GO-(HT)), and (iii) the low temperature conditions assisted with pre−exfoliation process (GO-(PreEx/LT)). Firstly, pre−exfoliated graphite (In case of pre−exfoliation of graphite) was prepared by adding graphite powder (3.0 g) into a flask containing 240 mL of deionized water and 120 mL of ethanol before sonicated in an ultrasonic bath for 3 h. After that, the sonicated graphite was isolated by using a centrifugal at 6000 rpm for 30 min. After that, the precipitate was dried in vacuum oven at 60ºC for 24 h. 2 g of dried graphite (or pre−exfoliated graphite) was mixed with 2 g of $NaNO_3$ and 90 mL of sulfuric acid at ~5 °C and stirred for 10 min. Next, 12 g of potassium permanganate ($KMnO_4$) was slowly added to the content at this temperature. The mixture was kept stirring at x °C (see Table S1) for further 6 h. After the content in the reaction flask turn dark green eventually, it was added with 200 mL of deionized water and kept under stirring at given temperature for 2 h. Next, the solution temperature was set to y °C (see Table S1) and then kept stirring for 2 h to ensure the completed reaction. After that, the content in the reaction flask was stirred at z °C (see Table S1) for 1 h. After the content in the reaction flask is turned into grayish purple brown, 55 mL of H_2O_2 (30 wt. %) was added to the residue to eliminate excess of $KMnO_4$. The reaction was kept stirring for further 30 min. Next, the content was diluted with deionized water. Then 10 mL of H_2O_2 (30 wt. %) was added again and kept stirring for another 10 min. Finally,

the content in the reaction flask was allowed to precipitate for 24 h, followed by removing of supernatant. After that, the precipitated product was washed with an aqueous solution of 10 wt. % of hydrochloric acid (100 mL) before separation by using a centrifugal at 6000 rpm for 15 min, for 3 times. The above washing processes were repeated using DI water, until pH value of the content was neutral. Finally, the product was isolated by using a centrifugal at 6000 rpm for 30 min before drying in a vacuum oven at 60 °C for 24 h.

TABLE S1: The conditions used in GOs synthesis

Samples	Pre-exfoliation	Temperature (°C)		
		x	y	z
GO-(LT)	×	5	10	20
GO-(HT)	×	15	40	90
GO-(PreEx/LT)	✓	5	10	20

For synthesis of N, S doped rGO, GO (120 mg) was sonicated in 500 mL of deionized water at room temperature for 1 h. Next, 8 mL of sodium hydroxide solution (0.80 M) was added to facilitate the dispersion of GO in the water. The solution was further sonicated at ~10 °C for 3 h. Next, 1 mL of thiourea solution (1 M) was dropwisely added to the solution and then stirred at room temperature for 3 h. After that, 4 mL of L-ascorbic acid solution (1.70 M), a reducing agent, was slowly added and the residue was kept stirring for 1.5 h at 70 °C. The black precipitate was filtered and subsequently washed with deionized water and ethanol several times before drying in a vacuum oven at 60 °C for 24 h. Finally, the product was calcined at 700 °C for 1 h under the argon atmosphere with heating rate of 1 °C/min.

S1.4: Fabrication of the dye sensitized solar cells (DSSC)

Fluorine doped tin oxide (FTO) substrates (25 x 25 mm^2), used for preparing both a photoanodes and cathodes, were firstly cleaned with HCl solution (0.2 M), deionized water and IPA in an ultrasonic bath at 60 °C for 30 min, 20 min, and 20 min, respectively. The FTO substrates were then dried with nitrogen gas and treated with plasma cleaner for 15 min.

To prepare a photoanode, compacted TiO_2 layer was applied into the cell configuration as hole blocking layer by applying 10 µL of the TiO_x sol−gel solution onto the FTO glass substrates via a rapid convective deposition technique, at moving speed of 600 µm/s. The TiO_x coated FTO was then calcined at 500 °C for 1 h (heating rate of 2 °C/min). Next, TiO_2 mesoporous layer (photoanode) was applied onto the TiO_x coated FTO substrate. 10 µL of titanium tetraisopropoxide (TTIP) and 0.5 mL of isopropanol were added to 0.10 g of TiO_2 (P25) powder, using a sonication process, at ~10 °C for 3 h. The various weight content (wt. %) of synthesized photoanode materials were mixed with P25 at this state. The mixture of paste (120 µL) was then applied onto the compacted TiO_2 layer coated FTO substrate by using a doctor blade technique, equipped with a microscope slide (90° ground edges, Marienfeld Superior, from Paul Marienfeld GmbH & Co. KG, Germany). The prepared electrode was then calcined at 500 °C for 1 h (heating rate of 10 °C/min). After that, the prepared photoanode substrates were sensitized by immersing them in a staining jar, containing a solution of the N719 (4 mg of N719 in co-solvents, 5 mL of anhydrous acetonitrile and 5 mL of anhydrous *tert*−butanol) at 80 °C for 30 min and at room temperature for 12 h, respectively. Finally, the dye absorbed photoanode was rinsed with anhydrous acetonitrile, followed by purging with nitrogen gas and then dried in an oven at 80 °C for 30 min.

The counter electrode was separately prepared by coating the pre-treated drilled (Ø 1.0 mm) FTO with Pt paste, using a doctor blade technique. The substrates were then annealed at 450 °C for 1 h (heating rate of 10 °C/min). The prepared Pt coated FTO counter electrode was then assembled with dye sensitized photoanode into a sandwich type cell, using a pre−cut (1.30 x 2.20 cm^2 rectangular) a sealing film (ethylene−acrylic acid copolymer, surlyn) as a frame. The cell was then sealed by applying a heat gun to melt the surlyn film. Next, 20 µL of the electrolyte solution (HI−30) was injected into the cells through a hole drilled in the counter electrode. The holes were plugged with glass cover with UV curable epoxy in order to avoid some leakage and evaporation of the liquid electrolyte inside the cells. Finally, the silver paste was applied on non−active area of the electrodes to prepare the contacts.

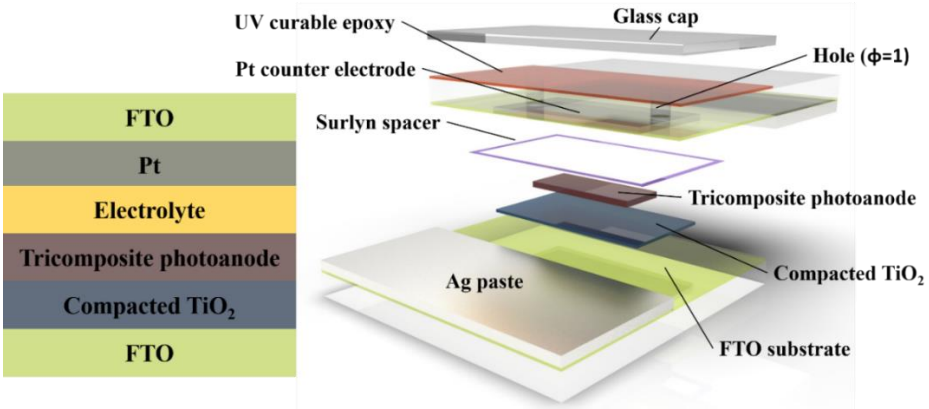

FIGURE S1: Device architecture of DSSC and its components.

S1.5: Characterizations

The crystal phase structures of synthesized photoanode materials were determined via X−ray diffractometer (PANalytical, X′Pert PRO) with Cu Kα radiation (λ = 0.15406 nm). The diffractometer was operated at 30 kV and 40 mA and the sample was scanned over a 2θ range of 0–80° at a scan rate of 0.01° s^{-1}. The morphology of the samples was examined using field emission scanning electron microscopy (FESEM) (FEI Nova Nanosem 450). The active sites density of $TiO_{2\{001\}}$ samples was determined via dye loading capacity.

The various $TiO_{2\{001\}}$ samples were stained with 3.4×10^{-4} M of dye (N719) solution and then desorbed the dye in 0.1 M of NaOH solution to exactly measure absorbed dye amount on TiO_2 surface by UV−Vis technique. The optical properties of the samples were investigated by using a UV−Vis−NIR spectrophotometer (Cary 5000, Agilent Technologies) in the spectral region of 190–900nm. X-ray photoelectron spectroscopy (XPS) measurements were performed using Kratos Axis Ultra DLD with Al K_α exciting radiation. The chemical structures of synthesized graphene were monitored by using a Fourier transform infrared spectrometer (FTIR) (Thermo Nicolet 6700) in a transparent mode. The sample was prepared by using a KBr technique and the FTIR spectra were scanned over the wavenumber ranging between 500 and 4000 cm^{-1}. The synthesized $TiO_{2\{001\}}$ and GO/rGO were analyzed by Raman spectrometer (NTEGRA Spectra, NTMDT) equipped with a 488 nm and 532 nm laser, respectively. Photoluminescence spectra of $TiO_{2\{001\}}$ samples were analyzed by using Perkin Elmer LS−55 spectrometer using 325 nm excitation wavelength.

Testing on power conversion efficiency of the DSSCs. Current density-voltage (J-V) characteristics of the various cells were measured by using the Keithley 2400 source meter under 1.5 AM. The light source was generated by a solar simulator (Newport 94011A model), equipped with a 1.5 G air mass filter. The active area of the DSSC was 0.5 × 1.0 cm^2. The external quantum efficiency (EQE) of DSSCs were measured by Newport Oriel QEPVSI-b 500 W xenon lamp. The operating condition includes the lamp power of 200 W, chopper frequency 8 Hz, and time constant of 30 s. The micrometer driven slit was adjusted to obtain the exposure intensity 1 W/cm^2 (0.4 cm^2 exposure area). The scanning wavelength was performed from 300 to 900 nm with the interval wavelength of 5 nm and waiting time of 5 s. Electrochemical impedance analysis (EIS) DSSC cells with various photoanodes was carried out in the dark condition at 0.75 V applied bias, using an impedance analyzer (Autolab-PGSTAT 302N). The impedance curves were recorded as Nyquist plots at 10 points per decade by superimposing 10 mV of AC signal onto the cell under potentiostatic mode with the frequency sweep from 1 MHz to 0.01 Hz.

S2: Characterization of $TiO_{2\{001\}}$ and N, S doped $TiO_{2\{001\}}$

The percentage of {001} facet (%S) of various $TiO_{2\{001\}}$ samples was calculated by using Raman data with Equation S1.

$$\%S = \frac{(Intensity\ at\ A_{1g})}{(Intensity\ at\ E_g)} \times 100 \qquad \text{Equation S1}$$

When E_g peaks is symmetric stretching vibration of O−Ti−O on {101} plane, while A_{1g} are antisymmetric bending of O−Ti−O in {001} plane.

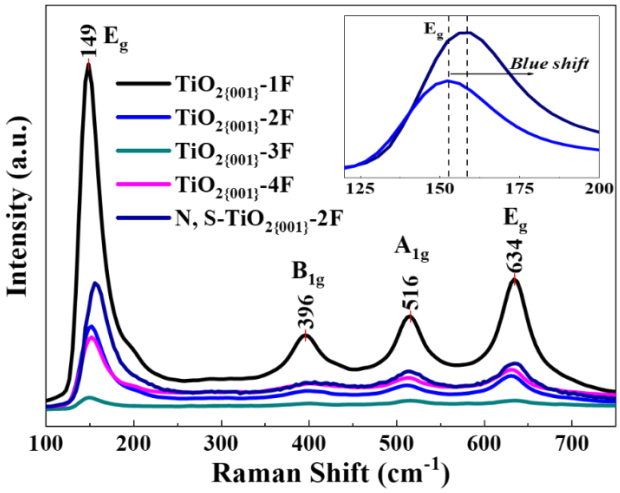

FIGURE S2: Raman spectra of various $TiO_{2\{001\}}$ and N, S-$TiO_{2\{001\}}$-2F.

The shallow trap and deep trap state of $TiO_{2\{001\}}$ synthesized by using different HF concentrations was conducted by the deconvolution of PL spectra.

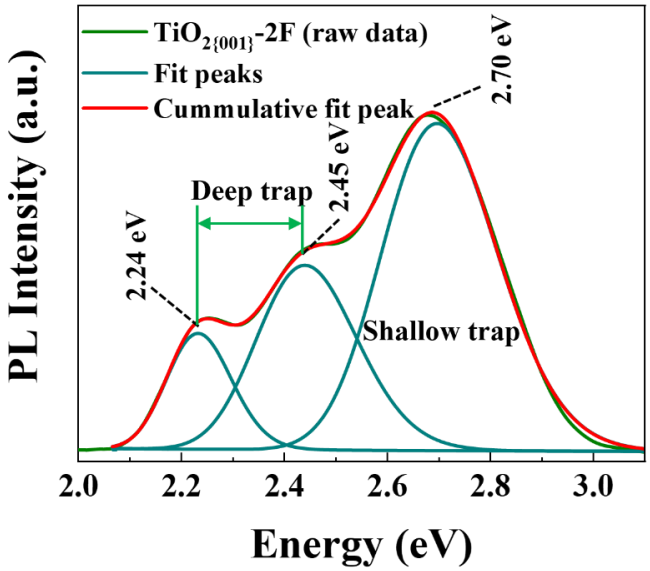

FIGURE S3: The deconvolution of PL spectrum of $TiO_{2\{001\}}$-2F by using Gaussian function.

Figure 4S shows the 1st (inset) and 2nd semicircle, which are correspond the charge transport dynamic at the Pt electrode and electron back reaction (recombination) at TiO_2/electrolyte interface. Due to high conductivity of Pt layer, thus, the Nyquist plot showed only the 2nd semicircle in the main text.

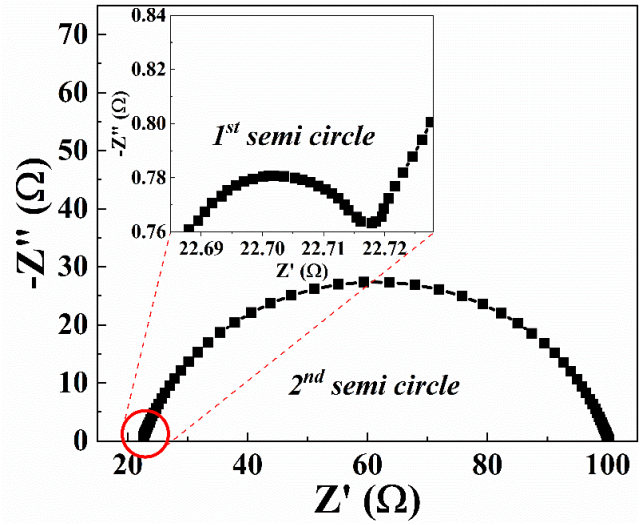

FIGURE S4: Nyquist plot of DSSC fabricated with P25 as photoanode.

In XPS analysis of N, S-$TiO_{2\{001\}}$-2F, the N 1s spectrum (Figure S5a) could be deconvoluted into three peaks at 395.6, 399.9 and 401.6 eV, corresponding the characteristic of N^{3-} (Ti−N), the oxidized nitrogen (N–O–Ti), and nitrogen in the form of Ti–N–O linkage, respectively [1−3]. In addition, The XPS of S 2p spectrum ((Figure S5b) could also be fit into two components at 166.6 eV and 168.3 eV, representing S^{6+} and S^{4+}, respectively [4].

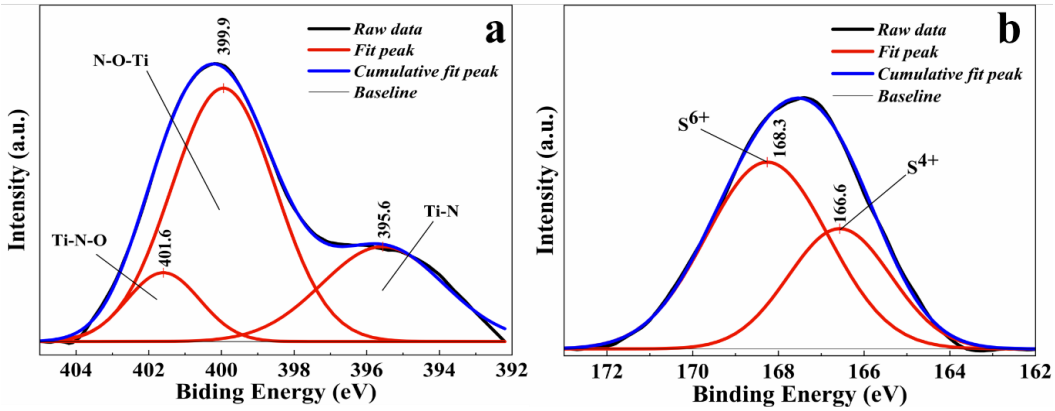

FIGURE S5: XPS spectra of N, S-$TiO_{2\{001\}}$-2F (a) N 1s and (b) S 2p.

S3: Characterization of GOs and N, S doped rGO

TABLE S2: The calculated d−spacing (d_{001}), grain size (L_{001}), number of layers (L_{001}/d_{001}), and diameter of stacking layers (D_A) of GO sheet with different synthesis conditions and N, S-rGO-(PreEx/LT).

Samples	Peak at (001) or (002)					Peak at (100)		
	2Θ (deg)	FWHM (deg)	d_{001} (nm)	L_{001} (nm)	Estimated NO. of layers (N_L)	2Θ (deg)	FWHM (deg)	D_A (nm)
GO-(LT)	12.20	0.94	0.72	8.47	13	42.5	0.9	19
GO-(HT)	12.92	3.38	0.68	2.36	4	42.7	2.1	8
GO-(PreEx/LT)	10.19	0.83	0.87	9.63	12	42.5	0.7	24
N, S-rGO-(PreEx/LT)	19.0−27.0	2.67−8.16	0.34−0.47	1.0−3.0	4−7	43.3	2.2	8

$$ORB\ (\%) = \frac{A_{(total)} - A_{(C=C)}}{A_{(total)}} \times 100 \qquad \text{Equation S2}$$

$A_{(total)}$ and $A_{(C=C)}$ are total peak area and peak area of C=C bond, respectively.

TABLE S3: The overall oxygen related bonds (ORB) of various GOs synthesized by different synthesis conditions.

Functional groups	Peak position (cm^{-1})			Integrated peak area (%)		
	GO-(LT)	GO-(HT)	GO-(PreEx/LT)	GO-(LT)	GO-(HT)	GO-(PreEx/LT)
α(C−O)	958−1041	949−1044	969−1042	43.52	43.43	32.81
β(C−O)	1154−1237	1242	1159−1221	5.7	0.35	1.28
γ(C−O)	1390	1383	1405	19.25	14.88	16.36
C=C	1564−1620	1582	1603	22.58	38.69	17.53
C=O	1719	1726	1731	8.94	2.66	32.02
		Percentage of ORB total (%)		77.42	61.31	82.47

 # The data were calculated using an Equation S2, excluding the OH peak at ~3400 cm^{-1}.

The successful incorporation of heteroatoms in graphitic lattice is clearly confirmed by XPS analysis (Figure S6a and S6b). The results showed that N 1s peak in the range of binding energy 397−402 eV, which could be deconvoluted into four components at 397.5 eV, 400.0 eV, 401.2 eV, and 402.8 eV, corresponding to pyridinic, pyrrolic, graphitic (or quaternary), and oxidized nitrogen species, respectively, as shown in Figure S8a [5−8]. Furthermore, the XPS of S 2p spectrum (Figure S8b) of N, S-rGO-(PreEx/LT) could be also deconvoluted into four components at 162.2−163.9 eV, 165.7 eV and 167.6 eV, representing to S $2p_{3/2}$, S $2p_{1/2}$, and oxidized sulfur groups, respectively [9−12]. The results show that the formation of graphitic nitrogen and S $2p_{3/2}$ (C−S−C) are the major species in graphene.

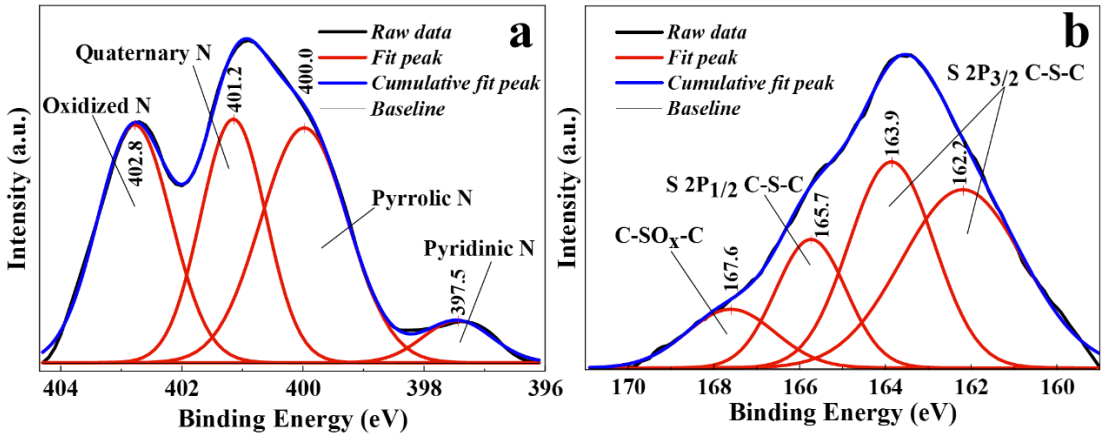

FIGURE S6: XPS spectra of N, S-rGO-(PreEx/LT) (a) N 1s and (b) S 2p.

S4: Photovoltaic performance of various photoanode materials

The N, S-$TiO_{2\{001\}}$-2F and N, S-rGO-(PreEx/LT) with different weight ratios in P25 were then utilized as a composite photoanode in DSSCs. Interestingly, as shown in Figure S7a and S7b, a significant enhancement in the J_{sc} up to 13.10 mA/cm^2 (6.55% PCE) and 13.77 mA/cm^2 (6.09% PCE) can be found in two devices containing 0.60 wt. % of N, S-$TiO_{2\{001\}}$-2F in P25 and 0.40 wt. % of N, S-rGO-(PreEx/LT) in P25, respectively. From these optimum contents, weight ratio between N, S-$TiO_{2\{001\}}$-2F and N, S-rGO-(PreEx/LT) was fixed at 0.60/0.40 by wt. (or 3/2 by wt.) and then this component was mixed with P25 for use as ternary composite photoanode system.

The different amount of mixture of N, S-$TiO_{2\{001\}}$-2F and N, S-rGO-(PreEx/LT) (3/2 by wt.) in P25 modified in DSSC as ternary composite photoanode were investigated. We found that the optimum amount loading amount of N, S-$TiO_{2\{001\}}$-2F/N, S-rGO-(PreEx/LT) (3/2 by wt.) was 1.00 wt. %, which showed the PCE of 8.62%, as seen in Figure S7c. The photovoltaic parameters were summarized in Table S4.

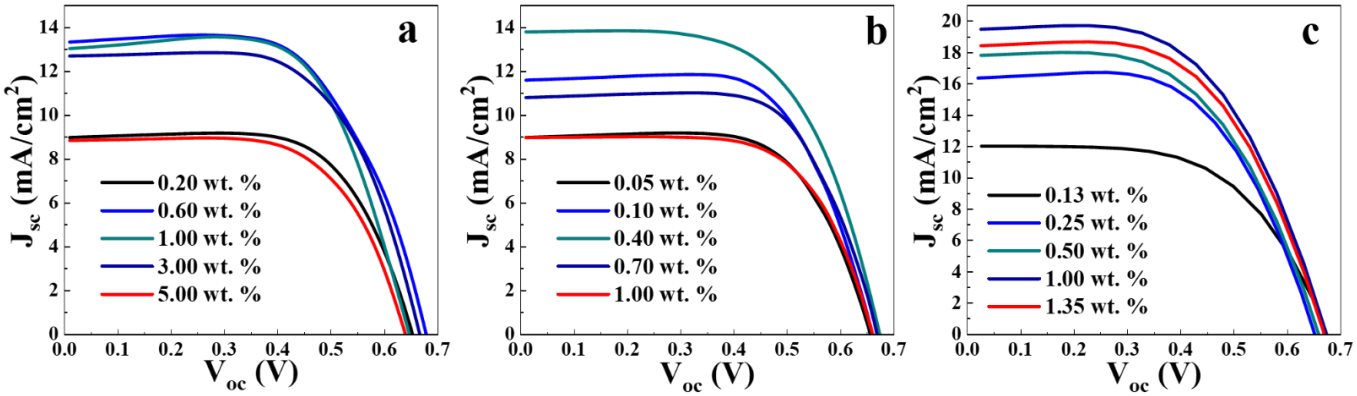

FIGURE S7: J−V curve of DSSCs fabricated with various content of composite photoanodes in P25 a) N, S-$TiO_{2\{001\}}$-2F and b) N, S-rGO-(PreEx/LT) (c) N, S-$TiO_{2\{001\}}$-2F/ N, S-rGO-(PreEx/LT) (3/2 by wt.).

TABLE S4: Short circuit current density (J_{sc}), open circuit voltage (V_{oc}), fill factor (FF), and power conversion efficiency (PCE) of DSSCs assembled with various composite photoanodes.

Photoanodes	Content in P25 (wt.%)	J_{sc} (mA/cm^2)	V_{oc} (V)	FF (a.u.)	PCE (%)	Stdv.
Pure P25	Pure	6.40	0.70	0.71	3.20	±0.183
N, S-$TiO_{2\{001\}}$-2F in P25	0.2	8.92	0.67	0.71	4.25	±0.112
	0.6	13.10	0.65	0.77	6.55	±0.109
	1.0	13.29	0.68	0.71	6.42	±0.229
	3.0	12.74	0.67	0.72	6.14	±0.315
	5.0	8.84	0.63	0.73	4.08	±0.333
N, S-rGO-(PreEx/LT) in P25	0.05	8.92	0.67	0.71	4.25	±0.158
	0.1	11.61	0.66	0.72	5.50	±0.212
	0.4	13.77	0.60	0.74	6.09	±0.209
	0.7	10.80	0.67	0.73	5.26	±0.313
	1.0	8.96	0.67	0.70	4.21	±0.329
Ternary composite photoanode	0.13	12.04	0.70	0.65	5.49	±0.146
	0.25	16.33	0.67	0.63	6.90	±0.183
	0.5	17.80	0.68	0.63	7.59	±0.133

1.0	19.47	0.69	0.64	8.62	±0.072
1.35	18.42	0.68	0.66	8.29	±0.223

References

[1] J. Wang *et al.*, "Origin of Photocatalytic Activity of Nitrogen-Doped TiO_2 Nanobelts," *J. Am. Chem. Soc.*, vol. 131, no. 34, pp. 12290–12297, 2009.

[2] G. Yang, Z. Jiang, H. Shi, T. Xiao, and Z. Yan, "Preparation of highly visible-light active N-doped TiO_2 photocatalyst," *J. Mater. Chem.*, vol. 20, no. 25, pp. 5301–5309, 2010.

[3] M. Zhang, J. Wu, D. Lu, and J. Yang, "Enhanced Visible Light Photocatalytic Activity for TiO_2 Nanotube Array Films by Codoping with Tungsten and Nitrogen," *Int. J. Photoenergy*, vol. 2013, p. 8, 2013.

[4] P. V. R. K. Ramacharyulu, D. B. Nimbalkar, J. P. Kumar, G. K. Prasad, and S.-C. Ke, "N-doped, S-doped TiO_2 nanocatalysts: synthesis, characterization and photocatalytic activity in the presence of sunlight," *RSC Adv.*, vol. 5, no. 47, pp. 37096–37101, 2015.

[5] T. Kondo *et al.*, "Observation of Landau levels on nitrogen-doped flat graphite surfaces without external magnetic fields," *Sci. Rep.*, vol. 5, p. 16412, 2015.

[6] R. Yadav and C. K. Dixit, "Synthesis, characterization and prospective applications of nitrogen-doped graphene: A short review," *J. Sci. Adv. Mater. Devices*, vol. 2, no. 2, pp. 141–149, 2017.

[7] M.-S. Lee, M. Park, H. Y. Kim, and S.-J. Park, "Effects of Microporosity and Surface Chemistry on Separation Performances of N-Containing Pitch-Based Activated Carbons for CO2/N2 Binary Mixture," *Sci. Rep.*, vol. 6, p. 23224, 2016.

[8] C. Guo *et al.*, "The Oxygen Reduction Electrocatalytic Activity of Cobalt and Nitrogen Co-doped Carbon Nanocatalyst Synthesized by a Flat Template," *Nanoscale Res. Lett.*, vol. 12, 2017.

[9] B. Quan *et al.*, "Single Source Precursor-based Solvothermal Synthesis of Heteroatom-doped Graphene and Its Energy Storage and Conversion Applications," *Sci. Rep.*, vol. 4, p. 5639, 2014.

[10] S. Gao *et al.*, "Facile preparation of sulphur-doped graphene quantum dots for ultra-high performance ultraviolet photodetectors," *New J. Chem.*, vol. 41, no. 18, pp. 10447–10451, 2017.

[11] T.-Y. Huang *et al.*, "Graphene Nanosheets/Poly(3,4-ethylenedioxythiophene) Nanotubes Composite Materials for Electrochemical Biosensing Applications," *Electrochimica Acta*, vol. 172, pp. 61–70, 2015.

[12] B. Anothumakkool, S. N. Bhange, S. M. Unni, and S. Kurungot, "1-Dimensional confinement of porous polyethylenedioxythiophene using carbon nanofibers as a solid template: an efficient charge storage material with improved capacitance retention and cycle stability," *RSC Adv.*, vol. 3, no. 29, pp. 11877–11887, 2013.